

Velocity dependence of the dynamic magnetic field acting on swift O and Sm ions

N. K. B. Shu, D. Melnik,* J. M. Brennan,† W. Semmler,‡ and N. Benczer-Koller

Department of Physics, Rutgers University, New Brunswick, New Jersey 08903

(Received 25 October 1979)

The hyperfine dynamic field acting on fast ions traversing polarized iron foils has been measured as a function of the ion velocity in the region $0.03 < v/Zv_0 < 0.06$ for Sm ions. The dynamic field increases with velocity but not linearly. The same conclusions were obtained from measurements on oxygen ions traversing thin iron foils or stopping in thick iron foils. All available data on dynamic-field measurements at ions with $8 < Z < 62$ traversing thin foils were examined and fitted to a single general form for the dynamic field. The region of validity of this parametrization of the dynamic field, as well as possible explanations of its origin, are discussed.

NUCLEAR REACTIONS $^{150,152}\text{Sm}(^{16}\text{O},^{16}\text{O}')^{150,152}\text{Sm}(2_1^+)$, $^{150,152}\text{Sm}(^{32}\text{S},^{32}\text{S}')^{150,152}\text{Sm}(2_1^+)$, and $^{16}\text{O}(\alpha, \alpha')^{16}\text{O}(3_1^-)$: $E_0 \sim 40$ MeV, $E_s \sim 70-80$ MeV, $E_\alpha = 17.55$ MeV; measured $W(\theta, B, \infty)$ through polarized iron; deduced $B_{\text{DYNAMIC}}(v)$; compiled existing data to obtain general parametrization for $B_{\text{DYNAMIC}}(v, Z)$.

INTRODUCTION

It has been known for many years that excited nuclei within ionized atoms traversing magnetic materials are subject to strong hyperfine interactions.¹ In order to obtain a consistent description of these interactions, it is helpful to separate the results of the various experiments according to the ion velocity through the solid.

Experiments on slow moving ions ($v/c < 0.01$) which eventually stop in polarized magnetic materials have shown that the ions experience a large magnetic interaction which results from the coupling between the magnetic moment of the nucleus and the magnetic field which acts on the moving ion.² This field was given the name of "transient field," and in the formulation of Lindhard and Winther³ was thought to vary inversely with the ion velocity. Many excited states nuclear magnetic moments were measured by this technique, but agreement with the model could only be obtained by arbitrary adjustment of parameters.⁴ In addition, these early experiments were subject to systematic uncertainties that were difficult to ascertain.

At very high velocities, ($v/Zv_0 \gg 1$ where $v_0 = e^2/\hbar$ is the Bohr velocity, and Z the atomic number of the ion), the ions can be assumed to be completely stripped and the interaction between the fast moving charge and the magnetized medium can be treated analytically in perturbation theory. The enhancement of the polarized electrons density around the moving ion was calculated classically by Sak and Bruno.⁵ They obtain the following expression for the magnetic field at the position of the moving ion:

$$B = 4\pi Z \frac{v_0}{v} \mu_B N_p, \quad (1)$$

where μ_B is the Bohr magneton and N_p the number of polarized electrons/cm³. Experiments on ^{12}C (Refs. 6 and 7) and ^{13}C (Ref. 8) nuclei and on fast polarized positive muons⁹ traversing iron plates, indicate that indeed at very high velocities the hyperfine field becomes vanishingly small. It must be emphasized here that even though the velocity dependence of the field at high velocities is the same as that predicted by the Lindhard-Winther theory, the magnitude of the interactions and the actual physical mechanisms responsible for them are very different.

At intermediate velocities the moving ion will be accompanied by bound atomic electrons and the nature of the interaction is considerably more complex as several competing mechanisms can in principle be responsible for the magnetic interactions between the ion and the solid. Recent studies^{1,6-8,10-13} have shown that excited nuclei traversing magnetic materials at relatively large velocities, $v/c > 0.01$, experience in fact a very much larger magnetic interaction than that predicted by the Lindhard-Winther model and that the magnetic field increases almost linearly with the velocity v of the ion. The Rutgers group developed a sensitive technique to test the velocity dependence of the hyperfine field.¹⁴ The moving ion is allowed to *traverse* a thin magnetic foil and made to stop in an interaction free environment. Thus the magnetic interaction acts only for the well-defined time during which the ion traverses the foil and by adjusting the foil thickness, the incoming and outgoing ion velocities

can be controlled. The thin foil idea was actually suggested in 1968 by Grodzins¹⁵ but had not been tested because it was believed at that time that the "transient field" was proportional to $1/v$ and therefore its magnitude would only be large enough for measurements to be carried out at the end of the ion trajectory.

The following expression for the field was proposed^{16,17} and generally used for practical purposes even though it had not been thoroughly tested:

$$B(v, Z) = a \left(\frac{v}{v_0} \right)^{p_v} (Z)^{p_z} \mu_B N_p, \quad (2)$$

where a is a constant and $p_v \approx p_z \approx 1$ are parameters that best fitted the early data for ions with $10 < Z < 48$. The field acting on fast ions was given the name of "dynamic field" to distinguish it from the interactions acting on very slow ions described by Lindhard and Winther. As the existence of the large dynamic field acting on *high* velocity ions was established, the advantages of the "thin magnetic foil technique" were fully realized.

The thin foil technique is particularly suited to the study of the ion-solid interaction because the results that emerge are essentially independent of the excited nucleus lifetime, of radiation damage in the stopping material which might affect the hyperfine interaction, and of a precise knowledge of the low energy ion stopping power. The last point is particularly relevant as the stopping powers of ions near the end of their range are not well known. In fact, strong oscillations have been observed both in the stopping powers of various ions from $Z = 6$ to $Z = 36$ in amorphous carbon¹⁸ and a similar ion-solid interaction has affected the measurement by the Doppler shift attenuation method of nuclear lifetimes¹⁹ of a particular ion (²²Na in the 3.34 MeV excited state) stopping in a complete range of stopping materials from $Z = 6$ to $Z = 83$. These oscillations have been generally attributed to atomic shell structure effects either in the slowing ion or in the stopping material. Van Middelkoop¹ has suggested a mechanism based on the creation of polarized holes in the s shells of the moving ion to explain the variations in the hyperfine interactions observed when light ions ($Z < 14$) stop in thick iron foils. They have analyzed the experimental data available in terms of the hyperfine field²⁰ due to the presence of an uncoupled but polarized $1s$ electron in C, N, and O ions, a $2s$ electron in Ne, Mg, and Si ions, and a $3s$ electron in Fe ions. They were able to fit all the above data with a single parameter thus strongly supporting the hypothesis that the dynamic fields

are of an atomic structure origin. In this work, they assume, however, that the dynamic field is linear in the velocity down to zero velocity. They caution therefore that this approach may have to be revised if the velocity dependence of the field is found to be different from linear.

The first systematic results on intermediate weight ions ($Z > 14$) were obtained in fast Se ions¹⁴ traversing *thin* iron and gadolinium foils and on fast Fe ions¹³ traversing iron foils; these data suggested that the parameters p_z and p_v in the expression for the dynamic field given by Eq. (2) differ from unity, and the best fits to the data yielded the somewhat crude results, $p_z = 1.5 \pm 0.5$ and $p_v = 0.5 \pm 1.0$.

Following these studies, "thin" target measurements were carried out on Pd and Cd isotopes²¹ in order to establish the Z dependence of the dynamic field for heavier ions. Furthermore, some of the data on the light ion experiments could also be used for this analysis even though the actual measurements were made with thick iron foils. The measurements had been carried out on ions entering the magnetic foil at a variety of initial velocities. The data were reanalyzed by subtracting the contribution obtained for the slowest ions from the effect measured for the faster ones. The analysis of these data seemed to suggest that the dynamic field dependence on the charge and velocity of the ion is indeed consistent with a linear behavior. However, later higher precision measurements on Pd ions and low velocity data on Sm ions contradicted this trend and suggested that if a unique field were to be responsible for the data observed for all isotopes for $6 < Z < 62$ and in the velocity range $0.02 < v/Zv_0 < 0.80$, then the dynamic field must be proportional to a lower power of the velocity.

It is clear that data with higher precision are required within a narrow velocity range, and for many Z before a correct description of the dynamic field can be proposed and therefore we undertook the measurement of the dynamic field acting on Sm and O ions as they traverse thin iron foils at varying but well-defined velocities.

EXPERIMENTAL PROCEDURES

The measurement of the dynamic field acting on fast moving ions traversing ferromagnetic materials is accomplished by observing in coincidence with back-scattered beam particles the precession of the angular correlation of gamma rays emitted in the decay of an aligned nuclear excited state whose magnetic moment is affected by the presence of the dynamic field (Fig. 1). The type of targets used and details of the technique

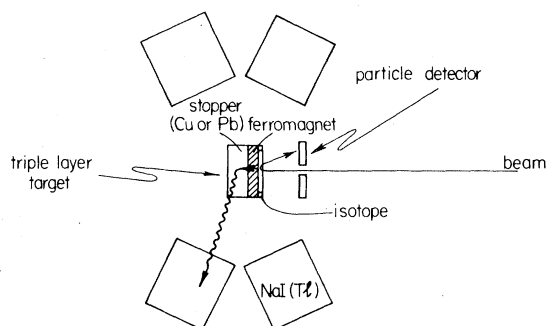


FIG. 1. Schematic of the experimental arrangement (not to scale) displaying the triple layer target and the γ -ray detectors. The recoiling ions traverse the ferromagnetic foil and stop in the interaction-free Cu or Pb backing.

have been extensively described in previous publications from this laboratory.^{13,14} The target consists of three layers: a relatively thin layer of the isotope under investigation (between 200 and 800 $\mu\text{g}/\text{cm}^2$ thick) evaporated on an iron foil (between 0.5 and 2.0 mg/cm^2) backed by a thick (>10 mg/cm^2) copper (or lead) foil. The target is placed between the pole pieces of a magnet which produces an external magnetic field of 0.03–0.05 T, which is used to polarize the iron foils either up or down perpendicular to the scattering plane. The direction of the external magnetic field is reversed periodically (every three to five minutes), according to a preset count in the particle detector window.

The exciting beam is scattered backward into an annular particle detector and the decay gamma radiation is detected in four 12.7 cm \times 12.7 cm NaI (Tl) detectors located 16.7 cm away from the target at the maximum slope angles of the particle-gamma angular correlation.

A. Sm ions

The first 2^+ states of both ^{150}Sm and ^{152}Sm at 335 and 122 keV, respectively, were Coulomb excited with oxygen and sulfur beams. The magnetic moment of the long-lived, $\tau = 2050$ psec state of ^{152}Sm , $\mu = 0.832 \pm 0.050$ n.m., was measured by Mössbauer spectroscopy.²² The magnetic moment $\mu = 0.78 \pm 0.07$ n.m. of the short-lived $\tau = 69.1 \pm 1.6$ psec state of ^{150}Sm was derived from the ratio $\mu(150)/\mu(152) = 0.936 \pm 0.060$ obtained by Ben Zvi *et al.*²³ from experiments on Sm ions recoiling in gas and the magnetic moment of ^{152}Sm derived from Mössbauer experiments.

The experiments on the Sm isotopes were carried out at a variety of initial velocities and for several thicknesses of the iron foil.

The long lifetime of the ^{152}Sm state had an im-

portant effect on the angular correlation in this experiment. Instead of the full angular correlation which was found for all states with picosecond mean lives, the correlation for ^{152}Sm ions stopping in copper was attenuated. A significant weaker attenuation in the angular correlation was obtained by using lead as a stopping material. It is assumed that the electric field gradients induced by radiation damage are responsible for the attenuation of the correlation, and that the radiation damage is different for copper and lead. The measured correlations for copper and lead backings are shown in Fig. 2. The result for the lead backing is very close to that which would be expected for complete alignment of the state after correction for the finite solid angle of the detectors. The normalized slope of the angular correlation at the angle of measurement $\theta_{\gamma} = \pm 67.5^\circ$ and $\pm 112.5^\circ$ was $|S| = (1/W)dW/d\theta|_{\theta_{\gamma}} = 2.86 \pm 0.10$ for the lead backing, and $|S| = 1.39 \pm 0.05$ for the copper backing. This effect was not observed for ^{150}Sm , and copper-backed targets were used for which $|S| = 3.03 \pm 0.10$.

It is interesting to note that even though the lifetimes of the two states vary by two orders of magnitude, the observed precession of the gamma-ray angular correlation in the dynamic field is comparable within statistical errors for the two nuclei when they move at the same average velocity through the magnetic foil and stop in an environment free of radiation damage, and more important, free of static magnetic hyperfine interactions. These would in fact be larger than the dynamic-field interaction for the long-lived ^{152}Sm state. This effect demonstrates vividly the power of the thin foil technique.

A beam-bending correction of $\Delta\theta = -0.09 \pm 0.06$ mrad corresponding to the effect of the 0.03 T external field on the incident and scattered beams

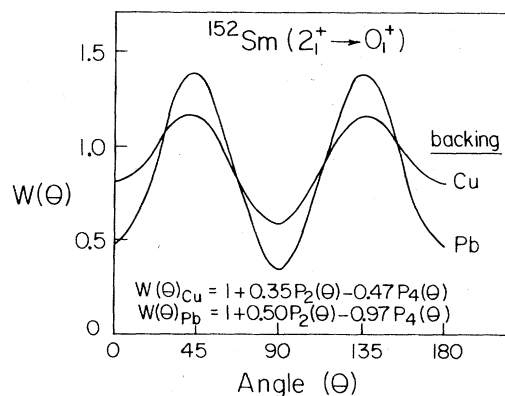


FIG. 2. Typical particle- γ angular correlation of ^{152}Sm ions for Cu and Pb backings. The four NaI(Tl) detectors were placed at angles $\theta = \pm 67.5^\circ$ and $\pm 112.5^\circ$.

was measured on a ^{150}Sm target evaporated on a Pb backing. The correction for the paramagnetic reduction²² of the applied field was neglected because it is uncertain, and in any case amounts to no more than 10–20% of the beam-bending correction. In the case of ^{152}Sm , the precession data were corrected for an additional angular shift of -1.2 mrad due to the precession of the moment of the long-lived 2_1^+ state in the external 0.03 T field.

The summary of all the data obtained on Sm isotopes is displayed in Table I.

B. O ions

The 6.131 MeV $J^\pi = 3^-$, $\tau = 26$ psec, $g = 0.55$ state²⁴ of ^{16}O was excited by inelastic α -particle scattering at a bombarding energy of 17.55 MeV. The scattered α particles were detected in an annular Si(Li) surface barrier detector at an angle $\theta_\alpha \approx 165^\circ - 172^\circ$. The excited nuclei traversed the ferromagnetic layer and stopped in an adjoining nonferromagnetic backing where they decayed. The de-excitation gamma-rays were detected in coincidence with the back-scattered α particles by the four 12.7 cm \times 12.7 cm NaI(Tl) detectors located at angles $\theta_\gamma = \pm 45^\circ$ and $\pm 135^\circ$ at which the measured angular correlation had its greatest slope $|S| = (1/W)(dW/d\theta) = 2.9$. The angular correlation was consistent with an 83% $m = 0$ magnetic substate population for the particular geometry involved (Fig. 3). The solid angle correction factors for the NaI(Tl) detectors were taken from the work of Little,²⁵ who calculated the relevant Q_b geometrical factors by the procedure developed by Black and Gruhle.²⁶

Several experiments were carried out. In the

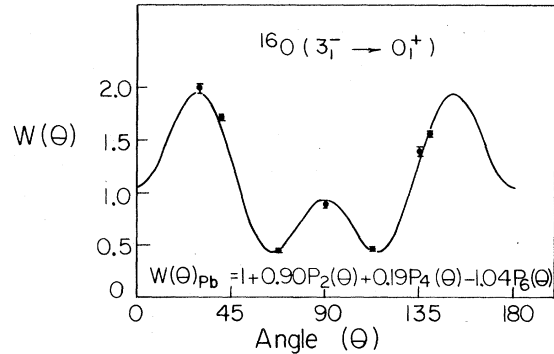


FIG. 3. Typical particle- γ angular correlation of ^{16}O for the $0^+ \rightarrow 3_1^- \rightarrow 0^+$ transition. The four NaI(Tl) detectors were placed at $\pm 45^\circ$ and $\pm 135^\circ$.

first series, targets of either $200 \mu\text{g}/\text{cm}^2$ WO_3 or $150 \mu\text{g}/\text{cm}^2$ SiO_2 were deposited on a $1.0 \text{ mg}/\text{cm}^2$ iron layer backed by $6 \text{ mg}/\text{cm}^2$ of Pb. For the second type of measurements, targets of $200 \mu\text{g}/\text{cm}^2$ WO_3 evaporated on a $6 \text{ mg}/\text{cm}^2$ iron backing thick enough to stop all recoiling oxygen ions were prepared.

A third type of experiment was necessary to determine the effect on the angular correlation due to the bending of the beam. This form of beam bending cannot be calculated from purely geometrical considerations when all the parameters of the nuclear reaction are not known.²⁷ In contrast to excitation by Coulomb excitation, in a nuclear reaction at energies much above the Coulomb barrier, the symmetry axis of the γ -ray angular correlation need not coincide with the recoil direction of the excited nucleus. Consequently the beam-bending effect was measured by observing the precession of the angular cor-

TABLE I. Summary of the experimental net precession angles $\Delta\theta$ observed for ^{150}Sm and ^{152}Sm isotopes. The parameter a_{lin} was calculated using Eq. (3). E_{in} , E_{out} , $(v/v_0)_{\text{in}}$, and $(v/v_0)_{\text{out}}$ are the energies and velocities of the moving ions as they enter and leave the ferromagnetic foil. L is the thickness of the foil and T is the time spent by the ion in the ferromagnetic foil.

	E_{in} (MeV)	E_{out} (MeV)	$(v/v_0)_{\text{in}}$	$(v/v_0)_{\text{out}}$	L ($\frac{\text{mg}}{\text{cm}^2}$)	T (psec)	$\Delta\theta$ (mrad)	a_{lin}^a
^{150}Sm	44.00	36.20	3.44	3.12	0.36	0.064	3.8(7)	88.6 ± 16.3
$\tau = 69.1(1.6)$ psec	44.21	32.81	3.45	2.97	0.55	0.100	4.9(4)	75.2 ± 6.5
$g = 0.390(35)$	34.19	24.59	3.03	2.58	0.55	0.115	5.1(4)	78.5 ± 6.6
	33.68	25.29	3.01	2.61	0.48	0.100	3.3(9)	57.1 ± 15.6
	33.38	11.73	3.00	1.78	1.50	0.375	17.8(9)	101.4 ± 5.4
	13.70	8.24	1.92	1.50	0.55	0.184	7.4(4)	115.0 ± 6.3
	13.19	9.39	1.88	1.60	0.36	0.124	3.9(5)	89.5 ± 11.5
^{152}Sm	39.3	14.3	3.13	1.86	1.58	0.364	20.5(8)	101.9 ± 4.0
$\tau = 2050$ psec $g = 0.416(25)$	34.8	11.8	3.04	1.78	1.58	0.393	19.2(7)	95.4 ± 3.4

^a a_{lin} was obtained by analyzing the data with the assumption that the dynamic field is given by $B(\psi, Z) = a_{\text{lin}} Z(\psi/v_0) \mu_B N_p$.

TABLE II. Summary of the net experimental precession angles $\Delta\theta$ for ^{16}O and ^{18}O isotopes and values of a_{lin} obtained as described in Table I.

Data	Ion	E_{in} (MeV)	E_{out} (MeV)	$\left(\frac{v}{v_0}\right)_{\text{in}}$	$\left(\frac{v}{v_0}\right)_{\text{out}}$	L (mg/cm ²)	T (psec)	$\Delta\theta$ (mrad)	$\Delta\theta/g$ (mrad)	a_{lin}^a	Ref.
I	^{16}O	8.07	3.17	4.51	2.87	1.0	0.160	-2.15(58)	-3.91(1.06)	100(27)	This work
II	^{16}O	8.07	0	4.51	0	2.24 ^b		-8.4(10)	-15.3(19)	168(22)	This work
III	^{18}O	3.78	0	2.90	0	1.5 ^b		-2.7(2)	9.3(9)	160(14)	11, 12
IV	^{16}O	1.597	0	2.14	0	0.91 ^b		-6.75(27)	-12.2(5)	346(19)	7
II-I	^{16}O	3.17	0	2.83	0	1.24			-11.4(21)		This work

^a a_{lin} was obtained by analyzing the data with the assumption that the dynamic field is given by $B(v, Z) = a_{\text{lin}} Z(v/v_0) \mu_B N_p$.

^bIn the cases where the O ions stopped in the iron foil the active thickness is the actual range of the ion.

relation with a target of 200 $\mu\text{g}/\text{cm}^2$ WO_3 on a 50 mg/cm^2 Pb backing. The beam bending was measured for external fields of 0.03 and 0.05 T. Whereas the purely geometric bending of the beam was calculated to be about -0.4 mrad, the actual beam bending turned out to be $\Delta\theta = -2.03 \pm 0.34$ mrad and $\Delta\theta = -3.05 \pm 0.44$ mrad for $B_{\text{ext}} = 0.03$ and 0.05 T, respectively.

The results of all the measurements on "thin" and "thick" iron targets are presented in Table II, and are compared to the data of Goldberg *et al.*⁷ on ^{16}O and by Forterre *et al.*¹¹ and Van Hienen¹² in a similar experiment on ^{18}O . In this latter work the 1.90 MeV $J^\pi = 2^+$, $\tau = 3.1$ psec²⁸ $g = -0.31$ (Refs. 11, 12, and 29) state of ^{18}O was also excited by inelastic alpha particle scattering but at lower energies, $E_\alpha = 7.4$ MeV, and the oxygen recoils stopped in the iron backing.

RESULTS

A. Sm ions

In the case where the dynamic field is assumed proportional to the first power of the velocity and atomic number of the ion [Eq. (2) with $p_v = p_z = 1$] $\Delta\theta$, the precession of the γ -ray angular correlation, is directly proportional to the thickness L of the magnetic foil as $\Delta\theta$ is given by

$$\begin{aligned} \Delta\theta &= -\frac{\mu_N}{\hbar} g \int B dt \\ &= -a_{\text{lin}} Z \frac{\mu_N g}{\hbar} (\mu_B N_p) \int_0^L \frac{v}{v_0} \frac{dx}{v} \\ &= -a_{\text{lin}} Z \frac{\mu_N g}{\hbar v_0} (\mu_B N_p) L. \end{aligned} \quad (3)$$

Figure 4 shows the value of the constant a_{lin} determined under the above constrictions for Sm ions plotted versus the average velocity of the ion

as it traverses the iron foil. The horizontal error bar indicates the range of velocities corresponding to the thickness of the foil. It is clear that a_{lin} is indeed not a constant, but decreases with the ion velocity suggesting that the simplified expression with $p_v \approx 1$ is not valid. Therefore, the data were fitted with a dynamic field described by Eq. (2) and the best values of the parameters p_v and p_z were obtained. For this analysis a precession angle $\Delta\theta$ is calculated taking into account the slowing down of each particular ion in the magnetic foil as well as the nuclear decays that might occur within the foil. The electronic stopping powers were taken from the tabulation of Northcliffe and Shilling³⁰ and a polynomial interpolation scheme was used in the analysis. The simple universal fit formula

$$\sum_n = \frac{1.7\epsilon^{1/2} \ln(\epsilon + e)}{1 + 6.8\epsilon + 3.4\epsilon^{3/2}}$$

in Lindhardt, Scharff, and Schiøtt units³¹ was

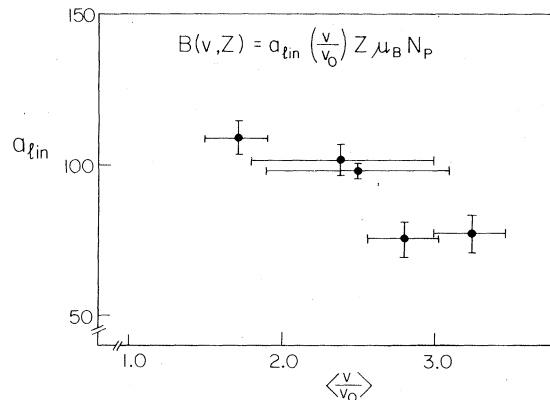


FIG. 4. Plot of the value of the constant a_{lin} , determined from Eq. (3), versus the average velocity of the Sm ion as it traverses the iron foil.

used for the nuclear stopping powers. The following integral was thus computed:

$$\begin{aligned} \frac{\Delta\theta}{g} &= -\frac{\mu_N}{\hbar} \int_0^T B(v, Z) e^{-t/\tau} dt \\ &= -\frac{\mu_N}{\hbar} \int_{E_i}^{E_f} B(v, Z) e^{-t/\tau} \left(\frac{1}{v} \frac{dE}{dx} \right), \end{aligned}$$

where T is the time the ion spends in the magnetic material, E_i is its initial velocity, and E_f is its energy as it leaves the magnetic foil. The actual calculation takes into account the thickness of the target, decays in flight, and the kinematic spread due to the finite solid angle subtended by the detector recording the exciting beam particles. The minimum chi square was searched and the best value for various parameters thus established. The best fit to the Sm data yielded $p_v = 0.50$ and $\chi^2 = 1.876$, but, of course, provides no information on p_z .

Several of the runs were performed in targets mounted on very thin iron foils. Under these circumstances one can assume that the ion velocity remains approximately constant through the foil and one may extract an average value for the dynamic field for that particular velocity

$$\langle B \rangle \approx \frac{\Delta\theta}{(\mu_N/\hbar)gT}.$$

Figure 5 shows the results obtained for Sm ions. The solid line represents the best fit to all existing data, and was obtained by the procedure described in subsection C below. A very similar study was done by King and Clark³² on ^{106}Pd . Their results are consistent with those obtained here.

B. O ions

Several conclusions can be drawn from the results presented in Table II. The most striking is the observation that the constants a_{lin} obtained from a fit to the data for the parametrization of the dynamic field with $p_v = 1$ are different by almost a factor of 2 for the thin (data I) and thick (data II and III) experiments. Since the dynamic field was found not to vary linearly with the velocity of the ion for Sm ions, it is no surprise that the same effect is observed for oxygen ions.

A rough estimate of the static hyperfine field acting on oxygen ions stopped in the iron foil can be obtained from the combined data on all oxygen isotopes. In the case of ^{18}O the precession of the angular correlation due to interaction with the static field is negligible in view of the short mean life of the 2_1^+ state. The long mean life of the 3^- state in ^{16}O , on the other hand, makes the precession of experiment II in the thick iron foil

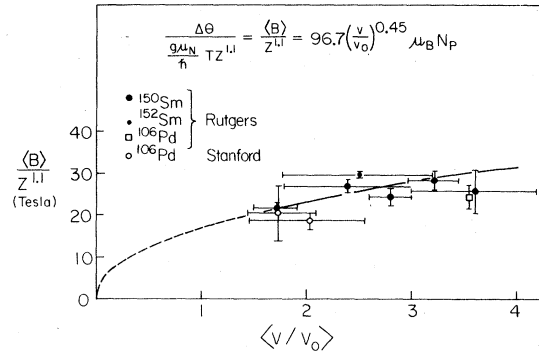


FIG. 5. Plot of the average value of the dynamic field $\langle B \rangle$ versus the transit velocity of Sm ions traversing iron foils. The solid line is a representation of the dynamic field according to Eq. (4) and the dotted line indicates the region where the formulation for Eq. (4) need not apply as no experimental data are available.

susceptible to both the influence of the dynamic and static hyperfine fields. If the precession corresponding to the high velocity portion (data I) of the range of the ion through the iron foil is subtracted from the data II, the resulting precession for ^{16}O ($\Delta\theta/g|_{\text{II}} - \Delta\theta/g|_{\text{I}}$) can be compared with the precession $\Delta\theta/g|_{\text{III}}$ obtained for ^{18}O for the same initial $v_i/v_0 = 2.9$ and final $v_f/v_0 = 0$ velocities. The precession of the angular correlation in just the static hyperfine field is given by

$$\Delta\theta = -\frac{\mu_N}{\hbar} g\tau B_{\text{static}} e^{-t_s/\tau},$$

where τ is the mean life of the state and t_s the time elapsed after creation of that state, or for the case of the thin foil experiments, the transit time of the ion in the iron layer before it stops.

An upper limit on the static field on ^{16}O ions stopping in iron can thus be extracted from

$$\begin{aligned} \left[\left(\frac{\Delta\theta}{g} \right)_{\text{I}} - \left(\frac{\Delta\theta}{g} \right)_{\text{II}} \right] - \left(\frac{\Delta\theta}{g} \right)_{\text{III}} &= \frac{\mu_N}{\hbar} g\tau B_{\text{static}} e^{-t_s/\tau} \\ &= (2.1 \pm 2.2) \text{ mrad}, \end{aligned}$$

giving B_{static} (oxygen) < 3.5 T. A similar analysis carried out by Gerber *et al.*³³ yielded $B_{\text{static}} < 9.0$ T. Data IV lists additional data obtained from a low velocity experiment on ^{16}O excited by the $^{19}\text{F}(\beta, \alpha)^{16}\text{O}$ reaction.³³ The effect observed in this experiment is even larger than that observed for the ^{18}O experiment at comparable velocities.

C. Other ions: Generalized formulation of the dynamic field

In order to obtain the best estimate of the dynamic-field dependence on the velocity and charge

TABLE III. Summary of the net experimental precession angles $\Delta\theta$ for ^{20}Ne , ^{24}Mg , ^{28}Si , ^{56}Fe , ^{82}Se , ^{106}Pd , ^{110}Cd , ^{194}Pt , and ^{148}Nd ions traversing thin iron foils and ^{82}Se ions traversing thin gadolinium foils. The original data for Ne, Mg, Si, and Ba ions were reanalyzed differentially as described in the text in order to simulate a "thin foil" experimental situation. For these data, L represents the effective target thickness corresponding to the chosen initial and final velocities of the ion, and T is the effective time spent by the ion at these velocities.

Ion	E_{in} (MeV)	E_{out} (MeV)	$(v/v_0)_{\text{in}}$	$(v/v_0)_{\text{out}}$	L (mg/cm ²)	T (psec)	$\Delta\theta$ (mrad)	Ref.
Ions traversing iron foils								
^{20}Ne	30.4	17.9	7.83	6.02	1.85	0.155	3.8(17)	34
$\tau = 1.0$ psec	30.4	13.9	7.83	5.31	2.42	0.214	5.0(15)	
$g = 0.54(4)$								
^{24}Mg	35.57	15.1	7.73	5.06	2.36	0.216	5.2(23)	34, 27
$\tau = 2.0$ psec	35.57	7.8	7.73	3.63	3.31	0.343	8.5(35)	
$g = 0.51(2)$	35.57	2.9	7.73	2.23	4.13	0.507	10.7(18)	
^{28}Si								
$\tau = 0.68$ psec	31.4	8.7	6.72	3.56	2.4	0.275	5.3(18)	35, 16
$g = 0.53(2)$	31.4	2.8	6.72	2.04	3.3	0.468	7.2(17)	
	31.4	0.8	6.72	1.13	3.85	0.675	8.0(18)	
^{56}Fe	65.0	23.7	6.83	4.14	2.3	0.247	8.9(17)	13
$\tau = 10$ psec	56.0	32.3	6.35	4.82	1.3	0.136	4.9(11)	
$g = 0.60(8)$	56.0	17.5	6.35	3.56	2.3	0.276	8.2(16)	
^{82}Se	53.0	42.5	5.10	4.57	0.5	0.060	1.6(14)	14
$\tau = 16.3$ psec	53.0	31.4	5.10	3.93	1.1	0.142	4.8(16)	
$g = 0.42$	53.0	24.3	5.10	3.46	1.54	0.212	6.8(16)	
	53.0	19.2	5.10	3.08	1.9	0.276	10.9(16)	
	53.0	11.0	5.10	2.33	2.6	0.429	13.7(15)	
^{106}Pd	47.4	21.5	4.24	2.86	1.36	0.226	7.3(8)	21
$\tau = 16.9(9)$ psec	42.0	18.1	4.00	2.63	1.36	0.244	8.3(12)	21
$g = 0.40(2)$	45.9	23.7	4.18	3.01	1.15	0.188	6.5(9)	31
	17.3	5.9	2.56	1.50	1.15	0.339	8.4(8)	31
	11.6	5.6	2.10	1.47	0.70	0.234	6.4(20)	31
^{110}Cd	45.0	16.7	4.06	2.48	1.6	0.291	7.5(20)	21
$\tau = 7.7(6)$ psec	45.0	12.0	4.06	2.10	2.0	0.394	11.7(20)	21
$g = 0.28(5)$								
^{134}Ba	12.1	7.4	1.91	1.50	0.49	0.171	5.4(18)	36
$\tau = 7.0$ psec	43.6	14.7	3.62	2.11	1.74	0.364	15.2(38)	36
$g = 0.43(5)^{21}$								
^{148}Nd	30.0	9.4	2.86	1.61	1.57	0.422	15.9(11)	37
$\tau = 123(3)$ psec								
$g = 0.33(4)$								
^{194}Pt	133.93	11.95	5.27	1.57	4.1	0.81	27.7(2.2)	38
$\tau = 60(4)$ psec	58.29	16.71	3.48	1.86	1.95	0.45	12.4(8)	38
$g = 0.274(25)$	35.72	13.62	2.72	1.69	1.44	0.389	9.2(8)	39
Ions traversing gadolinium foils								
^{82}Se	53.0	41.5	5.10	4.52	1.0	0.212	4.0(14)	14
	53.0	31.5	5.10	3.94	2.0	0.258	7.6(16)	
	53.0	18.7	5.10	3.04	3.6	0.526	20.4(44)	
	53.0	13.8	5.10	2.61	4.4	0.690	21.2(24)	

of the ion, all the existing data from this and other laboratories were collected (Table III) and analyzed. Only data obtained with "thin" iron foils were used. In the cases of Ne, Mg, Si, and Ba, however, the measurements were actually carried

out on targets deposited on thick iron backings in which the ions stopped. However, several data were obtained with ions at various initial energies. In order to evaluate the effects of the dynamic field acting on fast ions only, the data were

analyzed differentially as discussed in the Introduction.

The magnetic moments of all nuclear states used in the analysis are known from direct experiments such as measurements with radioactive sources in external fields or in known internal static hyperfine fields, with the exception of ^{28}Si where the theoretical value of $g(d_{5/2}^{-1}S_{1/2})$ was used.³⁴

In Fig. 6, the parameters a_{lin} obtained from these data analyzed in the context of a dynamic-field linear in the ion velocity are plotted. It is clear that with the exception of the Pt data, a_{lin} decreases with the increasing ion velocity for all ions, and increases slightly with the ion atomic number, in good agreement with the conclusions obtained from the O and Sm data.

The expression (2) for the dynamic field was simultaneously fitted to all tabulated "thin target" or equivalent data in order to evaluate the parameters a , p_v , and p_z . The best fit ($\chi^2 = 1.2$) yielded

$$B(v, Z) = (96.7 \pm 1.6) \left(\frac{v}{v_0} \right)^{0.45 \pm 0.18} Z^{1.1 \pm 0.2} \mu_B N_p. \quad (4)$$

Because a_{lin} for Pt appears to be much smaller than warranted by the trend displayed in Fig. 6, the Pt data were omitted from this fit. The solid line in Fig. 5 is a representation of this equation applied to the Sm data. The physical processes occurring at velocities $v/v_0 \approx 1.5$ are not well known and the above formulation need not apply (dotted line).

There is one glaring exception to the above fit: ^{194}Pt (Refs. 38 and 39) for which the observed angular precession is much smaller than the effect which would be predicted from the above parametrization of the field. No explanation of this anomaly can be offered yet. Recent ^{134}Ba measurements³⁶ in thick iron foils appear to be consistent with the assumption of a dynamic-field

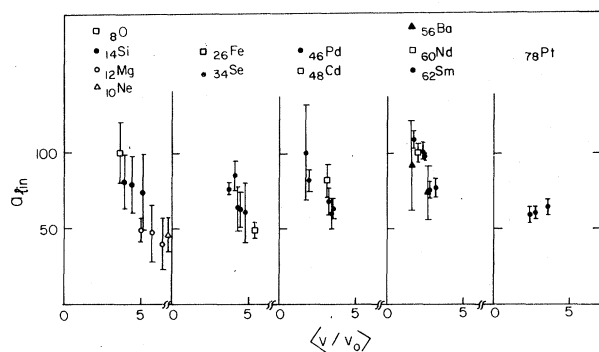


FIG. 6. Plot of the constant a_{lin} versus the average transit velocity for the data listed in Tables I, II, and III.

linear in the ion velocity. However, a differential analysis of these same data yield results compatible within statistical errors with the parametrization of the field given by Eq. (4) (Fig. 6).

DISCUSSION

The approach used in the data analysis involved fitting all available data displayed in Tables I, II, and III by a unique field $B(v, Z)$. This approach may be erroneous insofar as it is conceivable that light ions in which atomic structure effects are dominant would be subject to a different magnetic hyperfine interaction than the heavy ions where more complex electronic configurations might average out the sharp atomic features. Nevertheless, the Sm and O data confirm that the dynamic field is not simply proportional to the ion velocity.

Under these circumstances the very elegant analysis of the light nuclei by van Middelkoop *et al.*,¹ which exhibits clear atomic structure effects, ought to be revised even though the underlying ideas are undoubtedly correct. Furthermore, when the field is proportional to a complicated function of either velocity or atomic number, it is no longer possible to exhibit the features of the dynamic field by plotting the experimental data versus some common parameter; these can only be obtained from an analysis of the least square fit to a hypothetical model for the field. In fact, it may not even be possible to write $B(v, Z)$ as a product of two separable functions of v and Z . Nevertheless, the surprising results that all 40 independent experimental data points from $Z = 8$ to $Z = 62$ obtained in many laboratories can in fact be simultaneously fitted suggest that the dynamic field could indeed be described for practical purposes by a "universal" expression and hence could be used to measure the magnetic moments of other nuclei. However, as long as the microscopic origin of the field is not quantitatively described, the above fit of a generalized expression to the data should be considered more an accident than an accurate description.

A more physical approach leading to a parametrization of $B(v, Z)$ arises from the recent results of Dybdal *et al.*⁴⁰ They have measured the K vacancy fraction for Si ions moving in nickel foils and for O and F ions in iron and nickel foils. They have shown that the K vacancy fraction indeed increases with velocity, and that the dynamic magnetic field at the moving ion can be produced by a combination of spin exchange interactions between the moving ion and the magnetic material and capture-loss processes involving polarized

electrons. Furthermore, they have observed that the K vacancy production for O ions, contrary to that observed for other nearby ions such as F, does not remain proportional to the velocity as the velocity of the ion is reduced but stays approximately constant to very low velocity. This result is completely consistent with the present observations on the behavior of the dynamic field at O ions moving at very low velocity.

More quantitative K and higher shell vacancy production and dynamic-field data over the whole periodic table will be necessary to obtain a universal microscopic formulation for the dynamic field.

The "thin foil" technique is not the only approach to the study of the velocity dependence of the dynamic field. De Raedt *et al.*⁴¹ have recently made use of the line shape of the Doppler broadened gamma-ray line profile of ²⁸Si ions slowing down in magnetized iron foil. Their preliminary results indicate a dynamic-field proportional to the ion velocity. However, within the given statistical uncertainties in the measurements, the same data can be fitted equally well with the parametrization of Eq. (3). Another method which has been used to determine the velocity dependence of the magnetic field but is of limited scope involves the measurement of the interaction on very short-lived nuclei, and the recent experiment⁸ on ¹²C ions has confirmed the medium and high velocity behavior of the dynamic field. However, this technique is by its nature limited to the higher velocities. The "thin foil" technique, on the other hand, is more readily applicable to the measurement of magnetic moments. Its advantages have been extensively described in the Introduction and in previous publications, but its limitations should not be overlooked. Since neither the dependence of the dynamic field on velocity nor on atomic number is yet completely

understood from basic principles, the dynamic field should be applied with caution to absolute measurements of magnetic moments of excited levels:

(1) in ions which have no isotope with a known magnetic moment which could be used to calibrate the magnetic field,

(2) in a velocity range different from that used to calibrate the field in the case where a level with known magnetic moment is available.

It is interesting to note further that whatever parametrization of the dynamic field is chosen to reasonably fit the data for at least nearby nuclei, the best fit for each parametrization will yield the same magnetic moments for the unknown species to within 5%.²¹

One may conclude from these observations that whereas limited measurements of magnetic moments in well-chosen isotopes are possible, the greatest onus remains to establish the nature, or at least the behavior, of the dynamic magnetic field, either from basic principles or from semi-empirical analysis. The observation that the dynamic field is large and correlated with the velocity dependence of K -shell vacancy production does suggest that single polarized electrons play an important role and therefore that atomic structure effects must be taken into consideration. On the other hand, the fact that it is possible to fit all available data ranging over one order of magnitude in atomic number with a single expression for the dynamic magnetic field, and the expectation that ions moving through solids must occur with a broad charge distribution, suggest in turn that some average over many atomic configurations could be considered.

This work was supported in part by the National Science Foundation.

*Present address: Bell Laboratories, Murray Hill, New Jersey 07974.

†Present address: Nuclear Structure Laboratory, State University of New York, Stony Brook, New York, 11794.

‡Present address: Hahn-Meitner Institut, Berlin, West Germany.

¹G. Van Middelkoop, *Hyp. Int.* **4**, 238 (1978); this paper is a review of all the recent data and contains an extensive list of references.

²R. R. Borchers, J. D. Bronson, D. E. Murnick, and L. Grodzins, *Phys. Rev. Lett.* **17**, 1099 (1966); R. R. Borchers, B. Herskind, J. D. Bronson, L. Grodzins, R. Kalish, and D. E. Murnick, *ibid.* **20**, 424 (1968).

³J. Lindhard and A. Winther, *Nucl. Phys.* **A166**, 413

(1971).

⁴G. Hubler, H. W. Kugel, and D. E. Murnick, *Phys. Rev. C* **9**, 1954 (1974).

⁵J. Sak and J. Bruno, *Phys. Rev. B* **18**, 3437 (1978); J. Bruno and J. Sak, *Phys. Lett.* **A68**, 463 (1978); J. Bruno and J. Sak, *Phys. Rev. B* **19**, 3427 (1979).

⁶M. B. Goldberg, G. J. Kumbartzki, K.-H. Speidel, M. Forterre, and J. Gerber, *Hyp. Int.* **1**, 429 (1976); M. B. Goldberg, E. Konejung, W. Knauer, G. J. Kumbartzki, P. Meyer, K.-H. Speidel, and J. Gerber, *Phys. Lett.* **58A**, 269 (1976).

⁷M. B. Goldberg, W. Knauer, G. J. Kumbartzki, K.-H. Speidel, J. C. Adloff, and J. Gerber, *Hyp. Int.* **4**, 262 (1978).

⁸K. Dybdal, J. L. Eberhardt, and N. Rud, *Phys. Lett.*

- 64B, 414 (1976); K. Dybdal, J. L. Eberhardt, and N. Rud, *Hyp. Int.* **7**, 29 (1979).
- ⁹J. M. Brennan, N. Benczer-Koller, M. Hass, W. J. Kossler, J. Lindemuth, A. T. Fiory, D. E. Murnick, R. P. Minnich, W. F. Lankford, and C. E. Stronach, *Phys. Rev. B* **18**, 3430 (1978).
- ¹⁰M. Forterre, J. Gerber, J. P. Vivien, M. B. Goldberg, H.-K. Speidel, and P. N. Tandon, *Phys. Rev. C* **11**, 1976 (1975).
- ¹¹M. Forterre, J. Gerber, J. P. Vivien, M. B. Goldberg, and H.-K. Speidel, *Phys. Lett.* **55B**, 56 (1975).
- ¹²J. F. A. Van Hienen, Ph.D. thesis, Utrecht University, 1975 (unpublished).
- ¹³M. Hass, J. M. Brennan, H. T. King, T. K. Saylor, and R. Kalish, *Phys. Rev. C* **14**, 2119 (1976); J. M. Brennan, N. Benczer-Koller, M. Hass, and H. T. King, *ibid.* **16**, 899 (1977).
- ¹⁴J. M. Brennan, N. Benczer-Koller, M. Hass, and H. T. King, *Hyp. Int.* **4**, 268 (1978).
- ¹⁵L. Grodzins, *Hyperfine Structure and Nuclear Radiations*, edited by E. Matthias and D. A. Shirley (North-Holland, Amsterdam, 1968), p. 607.
- ¹⁶J. L. Eberhardt, R. E. Horstman, P. C. Zalm, H. A. Doubt, and G. van Middelkoop, *Hyp. Int.* **3**, 195 (1977).
- ¹⁷In the early publications a relativistic factor $R = 1 + (Z/84)^{2.5}$ was occasionally included in Eq. (2). However, as no fundamental argument supports its existence and it was often dropped from the equation when convenient, it will not be used here.
- ¹⁸C. P. Bhalla and J. N. Bradford, *Phys. Lett.* **27A**, 318 (1968).
- ¹⁹C. Broude, P. Engelstein, M. Popp, and P. N. Tandon, *Phys. Lett.* **39B**, 185 (1972).
- ²⁰H. Kopferman, *Nuclear Moments* (Academic, New York, 1958), p. 131.
- ²¹J. M. Brennan, M. Hass, N. K. B. Shu, and N. Benczer-Koller, *Phys. Rev. C* **21**, 574 (1980).
- ²²U. Atzmony, E. R. Bauminger, D. Froindlick, and S. Ofer, *Phys. Lett.* **26B**, 81 (1967).
- ²³I. Ben-Zvi, P. Gilad, M. B. Goldberg, G. Goldring, K.-H. Speidel, and A. Sprinzak, *Nucl. Phys.* **A151**, 401 (1970).
- ²⁴C. Broude, M. B. Goldberg, G. Goldring, M. Hass, M. J. Renan, B. Sharon, Z. Shkedi, and D. F. H. Start, *Nucl. Phys.* **A215**, 617 (1973).
- ²⁵W. A. Little, Ph.D. thesis, Stanford University, 1976 (unpublished).
- ²⁶J. L. Black and W. Gruhle, *Nucl. Instrum. Methods* **46**, 213 (1967).
- ²⁷J. L. Eberhardt, R. E. Horstman, H. W. Heeman, and G. van Middelkoop, *Nucl. Phys.* **A229**, 162 (1974).
- ²⁸Adopted average value quoted by A. M. Kleinfeld, K. P. Lieb, D. Werdecker, and U. Smilansky, *Phys. Rev. Lett.* **35**, 1329 (1975).
- ²⁹W. L. Randolph, N. Ayres de Campos, J. R. Beene, J. Burde, M. A. Grace, D. F. H. Start, and R. E. Wagner, *Phys. Lett.* **44B**, 36 (1973).
- ³⁰L. C. Northcliffe and R. F. Schilling, *Nucl. Data* **A7**, 233 (1970).
- ³¹J. Lindhard, M. Scharff, and H. E. Schiøtt, K. Dan. Vidensk. Selsk. Mat. Fys. Medd. **33**, 14 (1963).
- ³²H. T. King and D. L. Clark, *Bull. Am. Phys. Soc.* **23**, 961 (1978) and private communication.
- ³³J. Gerber, M. B. Goldberg, and K.-H. Speidel, *Phys. Lett.* **60B**, 338 (1976).
- ³⁴P. C. Zalm, A. Holthuisen, J. A. G. DeRaedt, and G. van Middelkoop, *Hyp. Int.* **4**, 347 (1978).
- ³⁵J. L. Eberhardt, G. van Middelkoop, R. E. Horstman, and H. A. Doubt, *Phys. Lett.* **56B**, 329 (1975).
- ³⁶J. L. Eberhardt and K. Dybdal, *Hyp. Int.* **7**, 387 (1980).
- ³⁷R. Kalish, J. A. G. DeRaedt, A. Holthuisen, W. A. Sterrenburg, and G. van Middelkoop, *Nucl. Phys.* **A311**, 3 (1978).
- ³⁸O. Häusser, B. Haas, D. Ward, and H. R. Andrews, *Nucl. Phys.* **A314**, 161 (1979).
- ³⁹R. Kalish, N. K. B. Shu, N. Benczer-Koller, A. Holthuisen, A. J. Rutten, and G. van Middelkoop, *Hyp. Int.* (to be published).
- ⁴⁰K. Dybdal, J. S. Forster, and N. Rud, *Phys. Rev. Lett.* **43**, 23 (1979).
- ⁴¹J. A. G. DeRaedt, A. Holthuisen, A. J. Rutten, W. A. Sterrenburg, and G. van Middelkoop, *Hyp. Int.* (to be published).